Chen et al. Nanoscale Research Letters (2016) 11:480
DOI 10.1186/s11671-016-1701-5

Nanoscale Research Letters

NANO EXPRESS Open Access

Ag-Decorated Localized Surface Plasmon-Enhanced Ultraviolet Electroluminescence from ZnO Quantum Dot-Based/GaN Heterojunction Diodes by Optimizing MgO Interlayer Thickness

Cheng Chen, Jingwen Chen, Jun Zhang, Shuai Wang, Wei Zhang, Renli Liang, Jiangnan Dai* and Changqing Chen

Abstract

We demonstrate the fabrication and characterization of localized surface plasmon (LSP)-enhanced n-ZnO quantum dot (QD)/MgO/p-GaN heterojunction light-emitting diodes (LEDs) by embedding Ag nanoparticles (Ag-NPs) into the ZnO/MgO interface. The maximum enhancement ration of the Ag-NP-decorated LEDs in electroluminescence (EL) is 4.3-fold by optimizing MgO electron-blocking layer thickness. The EL origination was investigated qualitatively in terms of photoluminescence (PL) results. Through analysis of the energy band structure of device and carrier transport mechanisms, it suggests that the EL enhancement is attributed to the increased rate of spontaneous emission and improved internal quantum efficiency induced by exciton-LSP coupling.

Keywords: ZnO, Quantum dots, Heterostructure, Localized surface plasmon

Background

Semiconductor nanoparticles termed quantum dots (QDs) have drawn wide attention in recent years as light-emitting source for light-emitting diode (LED) applications, whose emission spectrum with narrow linewidth can be tuned by changing the energy bandgaps with the variation in QD sizes and shapes [1–7]. Numerous experiments present in literature on the high-performance electroluminescence (EL) properties of LEDs based on CdS [8, 9], CdSe [10, 11], and PbS [12, 13] colloidal QD thin film. However, the widespread employment of heavy metal ions, particularly Cd and Pb, are a serious hazard to human health as well as to the environment [14]. Therefore, it necessitates alternative approaches for developing QD-LEDs with the heavy-metal free composition. Non-toxic ZnO QDs with a tunable direct wide bandgap and a large exciton binding energy of 60 meV at room temperature are very promising for solid-state LED applications [15, 16]. However, the main issue, the lack of high-quality and stable p-type doing of ZnO due to the strong self-compensation effect of native point defects such as zinc interstitial or oxygen vacancy, still remained. Thus, n-ZnO/p-GaN heterojunction LEDs are offered as an alternative approach due to the low lattice mismatch (1.9 %), similar bandgap energy between ZnO and GaN, and the same wurtzite crystal structure. Nevertheless, the spontaneous polarization of GaN [17–19] and the interfacial energy barrier between ZnO QDs and GaN will necessarily reduce the performance of the device, thus resulting the low EL efficiency of the device. To improve the EL efficiency of the LEDs, localized surface plasmon (LSP) has been introduced into n-ZnO/p-GaN LEDs to improve EL performance of the device. Recently, different metals like Au, Ag, and Pt have been observed to enhance the EL performance due to the enhancement of the internal quantum efficiency [20–26]. More recently, Lu et al. demonstrated a more than 30-fold EL enhancement of Al nanoparticle-decorated n-ZnO nanorod/p-GaN LEDs compared with that of the bare one [27]. Liu et al. showed the devices of LSP-enhanced ZnO/SiO_2 core/shell

* Correspondence: daijiangnan@hust.edu.cn
Wuhan National Laboratory for Optoelectronics, Huazhong University of Science and Technology, 1037 Luoyu Road, Wuhan 430074, Hubei, People's Republic of China

nanorod array/p-GaN heterostructure LEDs containing decorated with Ag nanoparticles. In comparison with the bare UV LEDs, the maximum enhancement ration of the Ag nanoparticle-decorated LEDs in EL is sevenfold [28]. However, many reports are mainly focused on the LSP-enhanced LEDs based on ZnO nanorods; there has been no literature concerning the LSP-enhanced EL emission in ZnO QD-based LED structure.

In this paper, we demonstrated the enhanced LSP-induced EL emission intensity in a n-ZnO QD/MgO/p-GaN LEDs. The MgO insulating layer is introduced primarily to modify the energy level alignment in the p-n heterojunction to confine the recombination. Meanwhile, there is a relatively small lattice mismatch of 6.5 % between GaN and MgO [29]. The maximum enhancement ration of the Ag nanoparticle-decorated LEDs in EL is 4.3-fold by optimizing MgO electron-blocking layer (EBL) thickness. To the best of our knowledge, this is the first work to observe the enhanced LSP-induced EL from ZnO QD-based p-i-n heterojunction LEDs to date. The EL origination and corresponding carrier transport mechanisms are investigated qualitatively in terms of photoluminescence (PL) results and energy band diagram in this study.

Methods

Commercially available p-type Mg-doped GaN epilayer with a c-plane sapphire base was used as the substrate. The carrier concentration of the p-GaN is approximately 4.53×10^{17} cm^{-3}. The MgO insulating layer directly gown on the pre-cleaned p-GaN/Al_2O_3 substrates by pulsed laser deposition (PLD) of an MgO ceramic target (99.99 % purity). Afterwards, colloidal Ag-NPs were spin-coated onto the MgO film. The colloidal Ag-NPs were synthesized in the presence of polyvinylpyrrolidone via a hydrothermal route [30]. ZnO QDs synthesized through a chemical-precipitation approach in the presence of $Zn(CH_3COO)_2{\cdot}2H_2O$ (99.0 % purity) and NaOH (96.0 % purity), and the reaction process proceeds in detail can be found in previous reports [31, 32]. The as-prepared ZnO QDs (20 mg/mL in ethanol) were uniformly spin-coated on the structure for 30 s at 3000 rpm to yield a complete and uniform ZnO QD thin film and then baked at 80 °C for 20 min to remove the solvent completely. At last, for the ohmic contact for n-ZnO and p-GaN layers, metal In monolayer and bilayer Ni/Au electrodes were made by electron beam evaporation. It is worth noting that because excitons were only located within the near field of the Ag-NPs' surface leading to resonant coupling. Therefore, a proper MgO thickness is of much importance for optimizing LED performance. The penetration depth (Z) of the Ag surface plasmon evanescent field into the MgO dielectric layer is calculated from the following equation [33]: $Z = \lambda/2\pi \left[\left(\varepsilon_d^{'} - \varepsilon_{\text{metal}}^{'}\right)/\varepsilon_d^{'2}\right]^{1/2}$, where $\varepsilon_d^{'}$ and $\varepsilon_{\text{metal}}^{'}$ represent the real parts of the dielectric constants of MgO and Ag, respectively, and Z can be calculated as $Z = 35$ nm at an emission wavelength of 360 nm. Therefore, the MgO thickness is controlled within 40 nm, the maximum luminescence enhancement can be obtained by varying MgO thickness, and this will be discussed in detail.

The morphologies and structures of the LSP-enhanced ZnO QD/MgO/p-GaN heterojunction were investigated by field emission scanning electron microscope (FESEM; FEI Nova NanoSEM). The as-prepared ZnO QDs were characterized by high-resolution transmission electron microscopy (HRTEM; FEI Tecnai G20). The current–voltage (I–V) characteristic curves of the devices were acquired using a Keithley 2420 sourcemeter. The PL measurements were recorded under a 325-nm He-Cd laser, and the emission was collected via a HORIBA Jobin-Yvon monochromator. EL spectra were recorded using homemade on-wafer testing and analyzing equipment including a prober system and a spectrograph.

Results and Discussion

As shown in Fig. 1a, Ag-NPs are evenly distributed throughout the MgO/p-GaN/sapphire film with an average particle size of ~40 nm and their shapes are nearly spherical. Figure 1b shows the extinction spectra of Ag-NPs, it can be seen that the resonance position of Ag-NP LSP is located at 400 nm, and there is considerable overlap between the broad Ag LSP resonance extinction band and the ZnO UV luminescence, indicating the probability of resonant coupling between Ag LSPs and ZnO excitions. The as-prepared ZnO QDs exhibit ball-like shape, and the mean particle size is 7 nm, as shown in the TEM image of Fig. 1c. It can be seen that the interplanar spacing in the crystalline petal is 0.26 nm in the inset of Fig. 1c, which correspond in the (002) planes of wurtzite ZnO, indicating the good crystallinity of the ZnO QDs. The PL spectra of the MgO/Ag-NP/ZnO composite films with various MgO thickness are shown in Fig. 1d. As the MgO thickness increased, the ZnO UV emission only gradually improved and no obvious variations are found in the visible emission. This phenomenon may be because the introduction of MgO interlay can suppress nonradiative Förster resonant energy transfer processes and thus leads to PL enhancement. Meanwhile, owing to the photon energy of ZnO UV emission is nearly consistent with the Ag-NPs' LSP resonance (LSPR) energy, so only the UV emission is efficiently enhanced. The PL integrated intensity reached

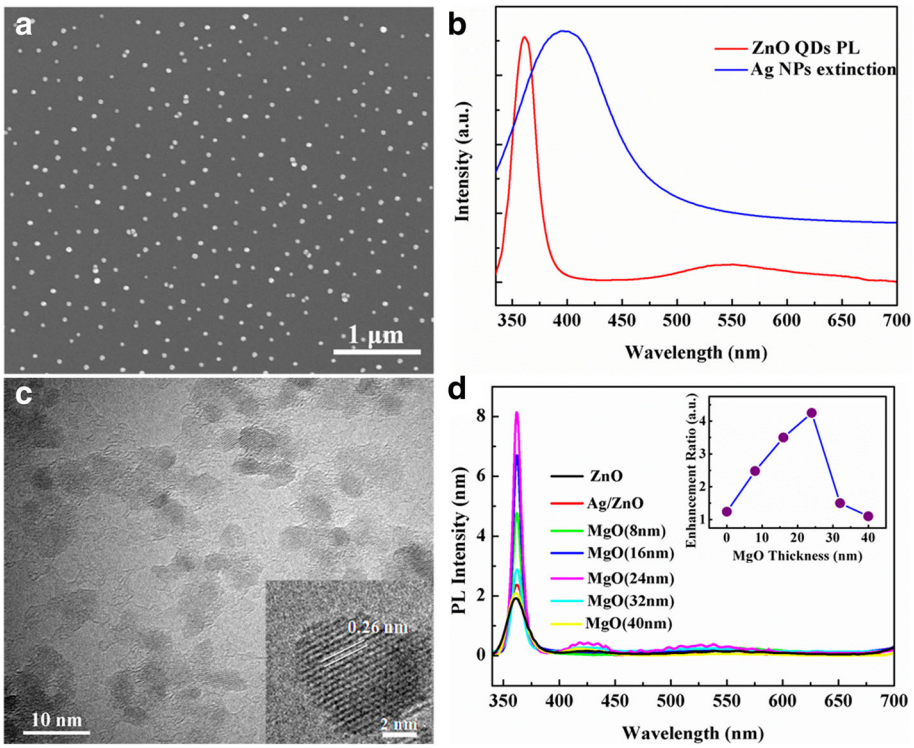

Fig. 1 **a** SEM image of the Ag-NPs spin-coated onto the MgO/p-GaN/sapphire film. **b** The extinction spectrum of Ag-NPs and the PL spectrum of ZnO QD film. **c** TEM image of the as-prepared ZnO QDs. The *inset* shows the typical HRTEM image. **d** PL spectra of bare ZnO film, Ag/ZnO film, and MgO/Ag-NP/ZnO composite films with various MgO interlayer thicknesses. The *inset* shows the variation of UV enhancement ration with the MgO interlayer thickness

maximum when the thickness of MgO layer is 24 nm, about 4.2-fold in comparison with that the device without Ag-NPs. However, with further increasing in MgO thickness, PL enhancement decreases sharply because of the evanescent wave nature of LSP. The corresponding variation of the enhancement ration of ZnO UV emission with the MgO thickness is illustrated in the inset of Fig. 1d. Thus, the MgO thickness of ~24 nm was selected as the insulating layer for the following LED device.

Figure 2a shows the schematic device structure of the LSP-enhanced ZnO QD/MgO/p-GaN LEDs. Figure 2b presents nonlinear I–V characteristic curve of the devices with and without Ag-NPs; it can be seen that both exhibit an obvious diode-like rectifying behavior with nearly the same turn-on voltage of about 8.0 V. The inset of Fig 2 shows the perfect I–V linear dependence exhibits good ohmic contact characteristic between a pair of Ni/Au or In electrodes. Compared with the LED without Ag-NPs, the LED with embedded Ag-NPs has

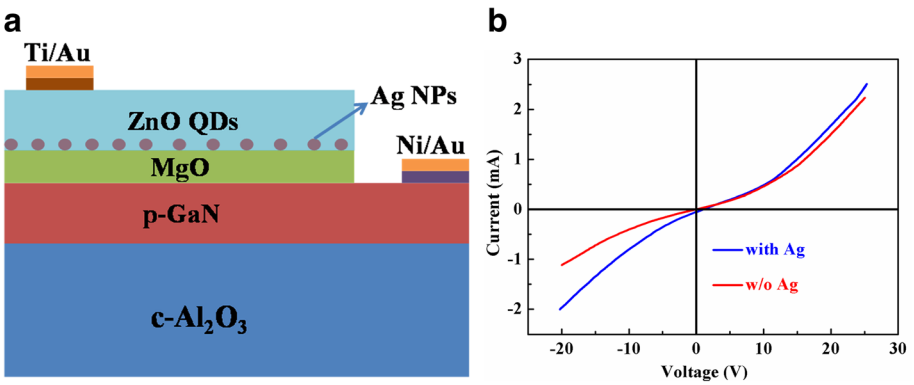

Fig. 2 **a** Schematic diagram of the LSP-enhanced ZnO QD/MgO/p-GaN LED device. **b** The I–V characteristic curve of the devices with and without Ag-NPs, and the *inset* shows the characterization of ohmic contacts on each part

relatively lower forward and reverse series resistance. The obvious decrease of the series resistance may result from the creation of more conductive paths owing to the introduction of Ag-NPs, thus resulting in a larger leakage current [34].

Figure 3a illustrates the EL spectra of the LSP-enhanced ZnO QD/MgO/p-GaN heterojunction LEDs with Ag-NPs under different forward injection currents covering from 0.7 to 2.8 mA. It is shown that the EL spectrum is composed of an evident UV emission located at 370 nm and a broad visible emission covering the range from 480 to 650 nm. With increasing of forward injection currents from 0.7 to 2.8 mA, the UV emission increases significantly and grows rapidly to be dominant, while the visible emission has been almost totally suppressed, which is similar to the previous literature [35]. However, the EL enhancement ration of the device as a function of the injection current exhibits an opposite tendency in Fig. 3b. A 4.3-fold EL enhancement is obtained under an injection current of 0.7 mA, and then, EL enhancement ration decreases rapidly with the increase of the injection current. This situation is a result of the screening effect of excess carriers, leading to a weakening of LSP-exciton coupling. The EL spectra of the ZnO QD/MgO/GaN LEDs with and without Ag-NPs were recorded at the same injection current of 0.7 mA (inset of Fig. 3b). Obviously, after insertion of Ag-NPs, only the UV emission is largely enhanced, namely, the radiative recombination is mainly confined in i-ZnO region by constructing p-i-n heterojunction. To further deeply understand the EL emission process, peak deconvolution analysis with Gaussian functions is illustrated in Fig. 3c. It is shown that peak deconvolution of the EL spectrum is composed of five individual peaks, located at 360, 370, 398, 420, and 550 nm. To verify the origination of each EL emission peak, the PL spectrum of the MgO/Ag-NP/ZnO composite films with MgO thickness of 24 nm is investigated by the peak deconvolution with Gaussian functions, which is in accord with the EL peak deconvolution data. Comparing the EL bands to the PL results in Fig. 3d, the five individual peaks mentioned above are successively ascribed to the near band emission (NBE) from the ZnO layer, that of the NBE emission from the GaN, that of interfacial radiative recombination, that of Mg acceptor-related emission of p-GaN, and that of the defect level (DL) emission from the ZnO [32].

In order to investigate the reason for the significant enhancement of UV emission, it is essential to understand the energy band structure of the LED and the

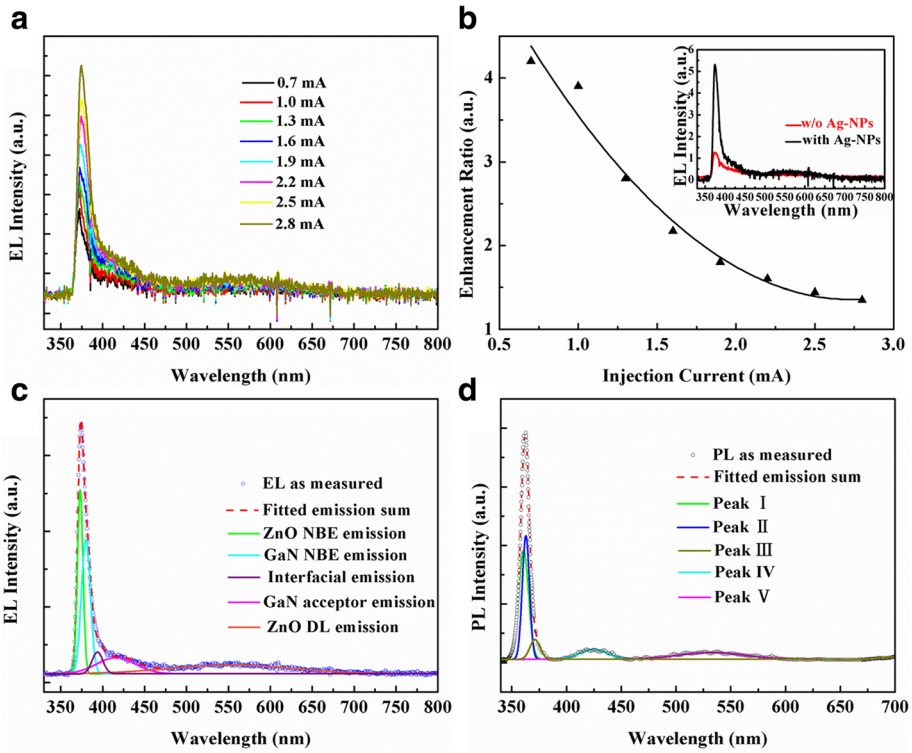

Fig. 3 **a** EL spectra of the LSP-enhanced ZnO QD/MgO/p-GaN LED under different forward injection currents. **b** The injection current dependence of the EL enhancement ration for the LED. The *inset* shows EL spectra of the n-ZnO QD/MgO/p-GaN heterojunction LEDs with and without Ag-NPs under an injection current of 0.7 mA. **c** Peak deconvolution of the EL spectra with Gaussian functions obtained at the injection current of 0.7 mA. **d** Gaussian deconvolution analysis of PL spectrum of the ZnO QD/MgO/p-GaN heterojunction with the MgO interlay thickness of 24 nm

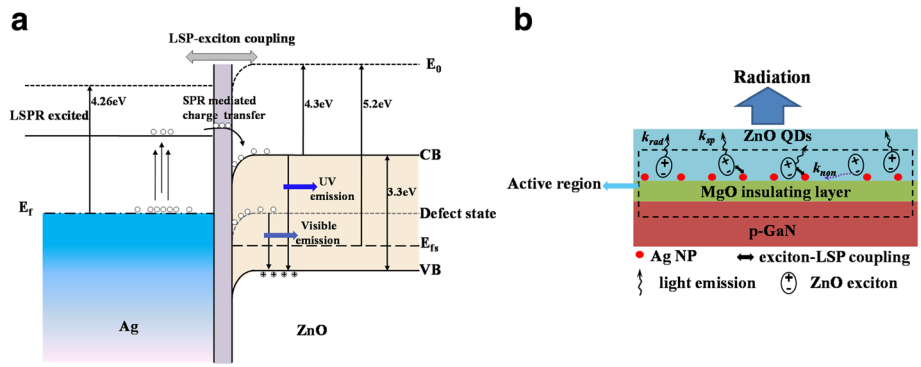

Fig. 4 **a** Energy band diagram of the LED showing LSP-exciton coupling. **b** The LSP-enhanced EL process schematic diagram. The k_{rad} and k_{non} denote the radiative and nonradiative recombination processes, respectively

carriers transfer process between the interfaces. Since the work function of ZnO is about 5.2 eV vs. NHE and its first electron affinity is about 4.3 eV vs. NHE, the work function of Ag is about 4.26 eV vs. NHE, as illustrated in Fig. 4a, this enables the electron transfer from the Ag to ZnO until the two systems achieve the uniform Fermi level, thus resulting in forming a strong polarization-induced local electromagnetic field due to the charge separation [36]. The oscillating electrons in the Ag-NPs can be excited to a high energy level by LSPR. The electrons with higher energy can subsequently transfer from the Ag-NPs to the conduction band of ZnO, causing an increased electron density in the conduction band of ZnO and then an enhanced ZnO NBE emission comparing to the device without Ag-NPs. In this course, high-rate recombination channel occurs between LSP and excitons, as shown in Fig. 4b. Meanwhile, the emerging exciton-LSP coupling rate k_{sp} is regarded as a faster recombination rate than the k_{rad} and k_{non} in ZnO [37]. Therefore, the rate of the spontaneous radiation is increased, leading to the improvement of internal quantum efficiency. It suggests that the EL enhancement is attributed to the increased rate of spontaneous emission and improved internal quantum efficiency induced by exciton-LSP coupling.

Conclusions

In conclusion, we have demonstrated the fabrication and characterization of LSP-enhanced n-ZnO QD/MgO/p-GaN heterojunction LEDs by embedding Ag-NPs into the ZnO/MgO interface. The maximum enhancement ration of the Ag-NP-decorated LEDs in EL is 4.3-fold by optimizing MgO electron blocking layer thickness. The EL origination was investigated qualitatively in terms of PL results. Through analysis of the band structure of device and carrier transport mechanisms, it suggested that the ZnO EL enhancement was attributed to the increased rate of spontaneous emission and improved internal quantum efficiency induced by exciton-LSP coupling. Due to the significant enhancement of UV emission of the device, it may open a door for pure high-performance ZnO QD-based UV LEDs.

Abbreviations

Ag-NPs: Ag nanoparticles; EBL: Electron-blocking layer; EL: Electroluminescence; LEDs: Light-emitting diodes; LSP: Localized surface plasmon; NBE: Near band emission; PL: Photoluminescence; QDs: Quantum dots

Acknowledgements

This work is supported by the National Basic Research Program of China (Grant No. 2012CB619302), the Science and Technology Bureau of Wuhan City (No. 2014010101010003), the Key Laboratory of infrared imaging materials and detectors, Shanghai Institute of Technical Physics, Chinese Academy of Sciences (Grant No. IIMDKFJJ-15-07), the National Natural Science Foundation of China (Grant No. 11574166), and the Director Fund of WNLO.

Authors' Contributions

All authors have contributed to the final manuscript of the present investigation. CC has defined the research topic, preparation, and characterization. SW, RL, JZ, WZ, JC, and CC participated in the preparation, and CC supervised the conceptual framework. CC wrote the manuscript, and JD provided important suggestions on the draft manuscript. All authors examined and approved the final manuscript.

Competing Interests

The authors declare that they have no competing interests.

Received: 31 August 2016 Accepted: 21 October 2016
Published online: 29 October 2016

References

1. Zhang Y, Xie C, Su H, Liu J, Pickering S, Wang Y, Yu W, Wang J, Wang Y, Hahm J, Dellas N, Mohney SE, Xu J (2011) Employing heavy metal-free colloidal quantum dots in solution-processed white light-emitting diodes. Nano Lett 11:329.
2. Lee K, Lee J, Song W, Ko H, Lee C, Lee J, Yang H (2013) Highly efficient, color-pure, color-stable blue quantum dot light-emitting devices. ACS Nano 7:7295.
3. Song W, Yang H (2012) Fabrication of white light-emitting diodes based on solvothermally synthesized copper indium sulfide quantum dots as color converters. Appl Phys Lett 100:183104.
4. Liang HW, Luo ZY, Zhu RD, Dong YJ, Lee JH, Zhou JY, Wu ST (2016) High efficiency quantum dot and organic LEDs with a back-cavity and a high index substrate. J Phys D Appl Phys 49:145103.
5. Shen HB, Lin QL, Wang HZ, Qian L, Yang YX, Titov A, Hyvonent J, Zheng Y, Li LS (2013) Efficient and bright colloidal quantum dot light-emitting diodes

via controlling the shell thickness of quantum dots. ACS Appl Mater Interfaces 5:12011.
6. Kong YL, Tamargo IA, Kim H, Johnson BN, Gupta MK, Koh T, Chin H, Steingart DA, Rand BP, Mcalpine MC (2014) 3D printed quantum dot light-emitting diodes. Nano Lett 14:7017.
7. Kwon B, Lee KG, Park TJ, Kim H, Lee TJ, Lee SJ, Jeon DY (2012) Continuous in situ synthesis of ZnSe/ZnS core/shell quantum dots in a microfluidic reaction system and its application for light-emitting diodes. Small 8:3257.
8. Jang E, Jun S, Jang H, Lim J, Kim B, Kim Y (2010) White-light-emitting diodes with quantum dot color converters for display backlights. Adv Mater 22:3076.
9. Gao XQ, Zhuo NZ, Liao C, Xiao LZ, Wang HB, Cui YP, Zhagn JY (2015) Industrial fabrication of Mn-doped CdS/ZnS core/shell nanocrystals for white-light-emitting diodes. Opt Mater Express 5:2164.
10. Kim TH, Cho KS, Lee EK, Lee SJ, Chae J, Kim JW, Kwon JY, Amaratunga G, Lee SY, Choi BL (2011) Full-colour quantum dot displays fabricated by transfer printing. Nat Photonics 5:176.
11. Likovich EM, Jaramillo R, Russell KJ, Ramanathan S, Narayanamurti V (2011) High-current-density monolayer CdSe/ZnS quantum dot light-emitting devices with oxide electrodes. Adv Mater 23:4521.
12. Chang LY, Lunt RR, Brown PR, Bulovic V, Bawendi MG (2013) Low-temperature solution-processed solar cells based on PbS colloidal quantum dot/CdS heterojunctions. Nano Lett 13:994.
13. Supran GJ, Song KW, Hwang GW, Correa RE, Scherer J, Dauler EA, Shirasaki Y, Bawendi MG (2015) High-performance shortwave-infrared light-emitting devices using core–shell (PbS–CdS) colloidal quantum dots. Adv Mater 27: 1437.
14. Lin Q, Shen H, Wang H, Wang A, Niu J, Qian L, Guo F, Li LS (2015) Cadmium-free quantum dots based violet light-emitting diodes: High-efficiency and brightness via optimization of organic hole transport layers. Org Electron 25:178.
15. Qiao Q, Li BH, Shan CX, Liu JS, Yu J, Xie XH, Zhang ZZ, Ji TB, Jia Y, Shen DZ (2012) Light-emitting diodes fabricated from small-size ZnO quantum dots. Mater Lett 74:104.
16. Omata T, Tani Y, Kobayashi S, Takahashi K, Miyanaga A, Maeda Y, Otsuka-Yao-Matsuo S (2012) Ultraviolet electroluminescence from colloidal ZnO quantum dots in an all-inorganic multilayer light-emitting device. Appl Phys Lett 100:061104.
17. Li S, Ware M, Wu J, Minor P, Wang Z, Wu Z, Jiang Y, Salamo GJ (2012) Polarization induced pn-junction without dopant in graded AlGaN coherently strained on GaN. Appl Phys Lett 101:122103.
18. Li S, Zhang T, Wu J, Yang Y, Wang Z, Wu Z, Chen Z, Jiang Y (2013) Polarization induced hole doping in graded AlxGa1− xN (x= 0.7~1) layer grown by molecular beam epitaxy. Appl Phys Lett 102:062108.
19. Li S, Ware ME, Wu J, Kunets VP, Hawkridge M, Minor P, Wang Z, Wu Z, Jiang Y, Salamo GJ (2012) Polarization doping: reservoir effects of the substrate in AlGaN graded layers. J Appl Phys 112:053711.
20. Zhang P, Li S, Liu C, Wei X, Wu Z, Jiang Y, Chen Z (2014) Near-infrared optical absorption enhanced in black silicon via Ag nanoparticle-induced localized surface plasmon. Nanoscale Res Lett 9:519.
21. Okamoto K, Niki I, Shvartser A, Narukawa Y, Mukai T, Scherer A (2004) Surface-plasmon-enhanced light emitters based on InGaN quantum wells. Nature Mater 3:601.
22. Kwon MK, Kim JY, Kim BH, Park IK, Cho CY, Byeon CC, Park SJ (2008) Surface-plasmon-enhanced light-emitting diodes. Adv Mater 20:1253.
23. Oh TS, Jeong H, Lee YS, Kim JD, Seo TH, Kim H, Park AH, Lee KJ, Suh EK (2009) Coupling of InGaN/GaN multiquantum-wells photoluminescence to surface plasmons in platinum nanocluster. Appl Phys Lett 95:111112.
24. Kim BH, Cho CH, Mun JS, Kwon MK, Park TY, Kim JS, Byeon CC, Lee J, Park SJ (2008) Enhancement of the external quantum efficiency of a silicon quantum dot light-emitting diode by localized surface plasmons. Adv Mater 20:3100.
25. Yang WF, Xie YN, Liao RY, Sun J, Wu ZY, Wong LM, Wang SJ, Wang CF, Lee AY, Gong H (2012) Enhancement of bandgap emission of Pt-capped MgZnO films: Important role of light extraction versus exciton-plasmon coupling. Opt Express 20:14556.
26. Lin CA, Tsai DS, Chen CY, He JH (2011) Significant enhancement of yellow–green light emission of ZnO nanorod arrays using Ag island films. Nanoscale 3:1195.
27. Lu JF, Shi ZL, Wang YY, Lin Y, Zhu QX, Tian ZS, Dai J, Wang SF, Xu CX (2016) Plasmon-enhanced electrically light-emitting from ZnO nanorod arrays/p-GaN heterostructure devices. Sci Rep 6:25645.
28. Liu WZ, Xu HY, Yan SY, Zhang C, Wang LL, Wang CL, Yang L, Wang XH, Zhang LX, Wang JN, Liu YC (2016) Effect of SiO_2 Spacer-layer thickness on localized surface plasmon-enhanced ZnO nanorod array LEDs. ACS Appl Mater Interfaces 8:1653.
29. Kato H, Sano M, Miyamoto K, Yao T (2003) Effect of O/Zn flux ratio on crystalline quality of ZnO films grown by plasma-assisted molecular beam epitaxy. J Appl Phys 42:2241.
30. Jiang T, Wang XL, Zhang L, Zhou J, Zhao ZQ (2016) Synthesis and improved SERS performance of silver nanoparticles-decorated surface mesoporous silica microspheres. Appl Surf Sci 378:181.
31. Toyama T, Takeuchi H, Yamaguchi D, Kawasaki H, Itatani K, Okamoto H (2010) Solution-processed ZnO nanocrystals in thin-film light-emitting diodes for printed electronics. J Appl Phys 108:084302.
32. Mo X, Long H, Wang H, Li S, Chen Z, Wan J, Feng Y, Liu Y, Ouyang Y, Fang G (2014) Enhanced ultraviolet electroluminescence and spectral narrowing from ZnO quantum dots/GaN heterojunction diodes by using high-k HfO_2 electron blocking layer. Appl Phys Lett 105:063505
33. Liu WZ, Xu HY, Zhang LX, Zhang C, Ma JG, Wang JN, Liu YC (2012) Localized surface plasmon-enhanced ultraviolet electroluminescence from n-ZnO/i-ZnO/p-GaN heterojunction light-emitting diodes via optimizing the thickness of MgO spacer layer. Appl Phys Lett 101:142101.
34. Zhang C, Marvinney CE, Xu HY, Liu WZ, Wang CL, Zhang LX, Wang JN, Ma JG, Liu YC (2015) Enhanced waveguide-type ultraviolet electroluminescence from ZnO/MgZnO core/shell nanorod array light-emitting diodes via coupling with Ag nanoparticles localized surface plasmons. Nanoscale 7: 1073.
35. Lin HY, Cheng CL, Chou YY, Huang LL, Chen YF, Tsen KT (2006) Enhancement of band gap emission stimulated by defect loss. Opt Express 14:2372.
36. Yin J, Zang YS, Yue C, Wu ZM, Wu ST, Li J, Wu ZH (2012) Ag nanoparticle/ZnO hollow nanosphere arrays: large scale synthesis and surface plasmon resonance effect induced Raman scattering enhancement. J Mater Chem 22:7902.
37. Zhang C, Xu HY, Liu WZ, Yang L, Zhang J, Zhang LX, Wang JN, Ma JG, Liu YC (2015) Enhanced ultraviolet emission from Au/Ag-nanoparticles@MgO/ZnO heterostructure light-emitting diodes: A combined effect of exciton- and photon- localized surface plasmon couplings. Opt Express 23:15565.